



HAL
open science

Solvent signal suppression for high-resolution MAS-DNP

Daniel Lee, Sachin Chaudhari, Gaël de Paëpe

► **To cite this version:**

Daniel Lee, Sachin Chaudhari, Gaël de Paëpe. Solvent signal suppression for high-resolution MAS-DNP. *Journal of Magnetic Resonance*, 2017, 278, pp.60-66. hal-02043257

HAL Id: hal-02043257

<https://hal.science/hal-02043257>

Submitted on 4 Oct 2021

HAL is a multi-disciplinary open access archive for the deposit and dissemination of scientific research documents, whether they are published or not. The documents may come from teaching and research institutions in France or abroad, or from public or private research centers.

L'archive ouverte pluridisciplinaire **HAL**, est destinée au dépôt et à la diffusion de documents scientifiques de niveau recherche, publiés ou non, émanant des établissements d'enseignement et de recherche français ou étrangers, des laboratoires publics ou privés.

1 Solvent signal suppression for high-resolution MAS-DNP

2 Daniel Lee^{1,2}, Sachin R. Chaudhari^{1,2}, Gaël De Paëpe*^{1,2}

3

4 ¹ Univ. Grenoble Alpes, INAC, F-38000 Grenoble, France. ² CEA, INAC, F-38000 Grenoble,
5 France.

6

7

8 **Abstract**

9 Dynamic nuclear polarization (DNP) has become a powerful tool to substantially increase the
10 sensitivity of high-field magic angle spinning (MAS) solid-state NMR experiments. The addition
11 of dissolved hyperpolarizing agents usually results in the presence of solvent signals that can
12 overlap and obscure those of interest from the analyte. Here, two methods are proposed to suppress
13 DNP solvent signals: a Forced Echo Dephasing experiment (FEDex) and TRAnsfer of Populations
14 in DOuble Resonance Echo Dephasing (TRAPDORED) NMR. These methods reintroduce a
15 heteronuclear dipolar interaction that is specific to the solvent, thereby forcing a dephasing of
16 recoupled solvent spins and leaving acquired NMR spectra free of associated resonance overlap
17 with the analyte. The potency of these methods is demonstrated on sample types common to MAS-
18 DNP experiments, namely a frozen solution (of *L*-proline) and a powdered solid (progesterone),

19 both containing deuterated glycerol as a DNP solvent. The proposed methods are efficient, simple
20 to implement, compatible with other NMR experiments, and extendable past spectral editing for
21 just DNP solvents. The sensitivity gains from MAS-DNP in conjunction with FEDex or
22 TRAPDORED then permits rapid and uninterrupted sample analysis.

23

24

25 **1. Introduction**

26 The combination of dynamic nuclear polarization (DNP) with high-resolution solid-state
27 nuclear magnetic resonance (ssNMR)¹ has led to previously-inaccessible insights into
28 biomolecules² as well as materials' surfaces.³ High resolution is obtained through the combination
29 of strong magnetic fields (> 5 T) and magic angle spinning (MAS⁴), and DNP is achieved through
30 suitable microwave (μ w) irradiation of unpaired electron spins, which permits the transfer of the
31 intrinsically large spin polarization of these spins to nearby nuclei.^{5,6} This polarization increase
32 experienced by the nuclei directly translates into signal(-to-noise) gains in NMR experiments.
33 Therefore, ssNMR experiments that would have required days, months, or even years of signal
34 averaging without DNP can now be performed in a small fraction of the time, making them readily
35 practicable. As such, two-dimensional (2D) correlation experiments eluding to internuclear
36 proximities, and thus atomic-level structures, can now be recorded in short experimental time for
37 nuclear spin-pairs using their low natural isotopic abundance (i.e., without isotopic enrichment),
38 for example ^{13}C - ^{13}C ,^{7,8} ^{13}C - ^{15}N ,⁹ and ^{29}Si - ^{29}Si ¹⁰ (with the natural abundance of ^{13}C , ^{15}N , and ^{29}Si
39 being 1.1%, 0.4%, and 4.7%, respectively).

40 Since DNP requires the presence of unpaired electron spins, which are not present in most
41 samples, it is usually necessary to introduce exogenous "polarizing agents" containing these spins

42 to the analyte. For efficient DNP, and also subsequent ssNMR experiments, these polarizing agents
43 should be homogeneously distributed in an optimal concentration.¹¹ To achieve a homogeneous
44 distribution, exogenous polarizing agents are normally dissolved in a glass-forming solvent or
45 solvent mixture, which is then added to the analyte. Although glassing-matrices with beneficial
46 properties for MAS-DNP experiments,¹² such as glycerol/water,¹ dimethylsulfoxide/water,¹³
47 1,1,2,2-tetrachloroethane,¹² 1,1,2,2-tetrabromoethane,¹² and ortho-terphenyl,¹⁴ have all been
48 successfully utilized, they all contain NMR-active nuclei and therefore exhibit resonances that can
49 overlap with signals of interest from the analyte in acquired spectra. ¹³C ssNMR is particularly
50 important since it is crucial for studies of organic molecules (biomolecules, pharmaceuticals, etc.),
51 but also material science (organic-inorganic hybrids, polymers, molecular organic frameworks,
52 etc.). So the employment of glycerol, dimethylsulfoxide (DMSO), 1,1,2,2-tetrachloroethane
53 (TCE), 1,1,2,2-tetrabromoethane (TBE), and ortho-terphenyl (OTP) can be detrimental as they all
54 contain carbon nuclei. The most ubiquitous mixture is glycerol/water, specifically glycerol-
55 d₈/D₂O/H₂O (60/30/10; v/v/v), since it can be used with the vast majority of systems, acts as a
56 cryoprotectant, and forms a good glass at temperatures < 140 K.¹⁵ Low temperatures (< 200 K) are
57 conventionally used for DNP as they result in increased DNP efficiency¹⁶ due to better glasses and
58 longer spin relaxation times and coherence lifetimes.¹¹ To reduce the problem of spectral overlap
59 for MAS-DNP studies involving ¹³C ssNMR, ¹³C-depleted deuterated glycerol^{17,18} has been used.
60 However, this is an expensive work-around (¹²C₃ (99.95 %), D₈ (98 %), ~\$650 per gram at the
61 time of writing). Some sample preparation procedures, such as incipient wetness impregnation³
62 and the Matrix-Free^{7,19} approach, can limit the amount of DNP matrix used, while still retaining
63 DNP efficiency. However, these procedures can still result in significant solvent signals and are
64 not suitable for all possible analytes.

65 Spectral editing can be used to remove unwanted signals in NMR spectra. Spectral editing
66 involves the use of data processing techniques and/or acquisition methods to retain only the desired
67 signals.^{20,21} The use of specific NMR pulse sequences, for example, can allow the favoring of
68 certain signals over others, usually by modifying the intensity or phase of these others. In solution-
69 state NMR, this type of spectral editing is routinely used to remove solvent signals. For the
70 suppression of solvent resonances in solution-state ¹H NMR, various pulse sequences have been
71 proposed²¹ and these generally involve the selective saturation of signals at a particular finite
72 frequency, which corresponds to that of the solvent signals. However, this method is not suitable
73 for the present problem since solution-state solvent signals are narrow and signals that are
74 overlapping with (i.e., at the same frequency as) these solvent signals are not recovered. The ¹³C
75 NMR signals arising from solvent molecules in a frozen glass are (heterogeneously) broad
76 (typically ~5-10 ppm) and thus there could be many ¹³C resonances from the analyte within the
77 same frequency range. Therefore, it is necessary to suppress the solvent signals in a different
78 manner. Spin-echoes have been employed for this purpose,²² whereby a long MAS-synchronized
79 delay is added either side of a refocusing π -pulse. However, this method is only suitable if the
80 solvent has a much shorter time constant for transverse signal decay under a refocusing echo, T_2' ,
81 than the analyte.

82 Since deuterated solvents are commonly used for DNP matrices so that an overall ¹H
83 concentration roughly equivalent to the ¹H concentration in glycerol-d₈/D₂O/H₂O (60/30/10; v/v/v)
84 is obtained as this gives good DNP efficiency,¹⁵ this then brings a difference between analyte and
85 solvent. It is this difference that can be exploited. For the glycerol/water DNP matrix, the glycerol
86 is conventionally fully deuterated (i.e., glycerol-d₈) and thus all of its carbon nuclei are directly
87 bonded to at least one ²H (see inset in Figure 3). Therefore, spectral editing that involves triple-

88 resonance ($^1\text{H}/^{13}\text{C}/^2\text{H}$) experiments could potentially be used in a similar manner to those already
89 used for spectral editing of isotopically-labeled biomolecules through triple-resonance
90 ($^1\text{H}/^{13}\text{C}/^{15}\text{N}$) experiments.²³ There, REDOR²⁴-type experiments were used to recouple the ^{13}C - ^{15}N
91 dipolar interaction, which is decoupled under MAS, so that ^{13}C nuclei in the near proximity (within
92 one bond) of ^{15}N nuclei would be dephased, leaving only ^{13}C signals in the resulting NMR
93 spectrum of sites that are distant from nitrogen-containing moieties. However, REDOR is used to
94 recouple spin-1/2 nuclei, and is thus not appropriate for the work here since ^2H is a spin-1 nucleus.
95 For the recoupling of ^{13}C with quadrupolar nuclei (spin $> 1/2$), TRAPDOR NMR²⁵ can be used.
96 Herein, a spectral editing approach is proposed to remove signals associated with the DNP matrix.
97 Two methods are presented that reintroduce the heteronuclear dipolar interaction to ^2H spins
98 during a “dephasing period” so that only resonances from spins that are not coupled to ^2H remain
99 in the resulting spectrum. The utility of both methods is presented firstly on a frozen solution of
100 *L*-proline, and then secondly on powdered progesterone. The results demonstrate that the presented
101 technique, combined with MAS-DNP, produces solvent-free spectra with large sensitivity, thus
102 facilitating the fast spectral assignment of analytes.

103

104 **2. Materials and methods**

105 2.1. Preparation for DNP experiments

106 A solution of 2 M *L*-proline at natural isotopic abundance, 10 mM AMUPol,²⁶ and
107 glycerol- d_8 /D₂O/H₂O (60/30/10; v/v/v) was prepared and a 20 μL aliquot of this was inserted into
108 a 3.2 mm outer-diameter sapphire sample rotor, which was subsequently sealed with a silicone
109 plug and closed with a zirconia drive cap. The progesterone sample was prepared by gently hand-

110 grinding the white solid and slowly adding 10 mM AMUPol and glycerol-d₈/D₂O/H₂O (60/30/10;
111 v/v/v) solution until the powder appeared slightly wet. The damp powder was then fully packed
112 (~30 mg) into a 3.2 mm outer-diameter thin-wall zirconia sample rotor, which was then sealed
113 only with a Vespel drive cap. The sample-containing rotor was inserted into a pre-cooled (~100
114 K) MAS-DNP triple-resonance (¹H/¹³C/²H) NMR probe and pneumatically spun to the required
115 rotation rate, ν_r , using cold nitrogen gas. Under these MAS conditions, a few watts of microwave
116 (μ w) irradiation at approximately the Larmor frequency of the unpaired electron spins of AMUPol
117 (~ 264 GHz) are applied to the sample, which enables the transfer of the large spin polarization of
118 the unpaired electrons to nearby nuclei. For ¹H, ¹H–¹H dipolar couplings facilitate the equilibration
119 of this hyperpolarization throughout the whole spin system. The *L*-proline, progesterone, glycerol-
120 d₈ (98% in D atoms) and D₂O (> 99% in D atoms) were standard commercial reagents, and the
121 AMUPol biradical polarizing agent was purchased through SATT Sud Est, Marseille, France.

122

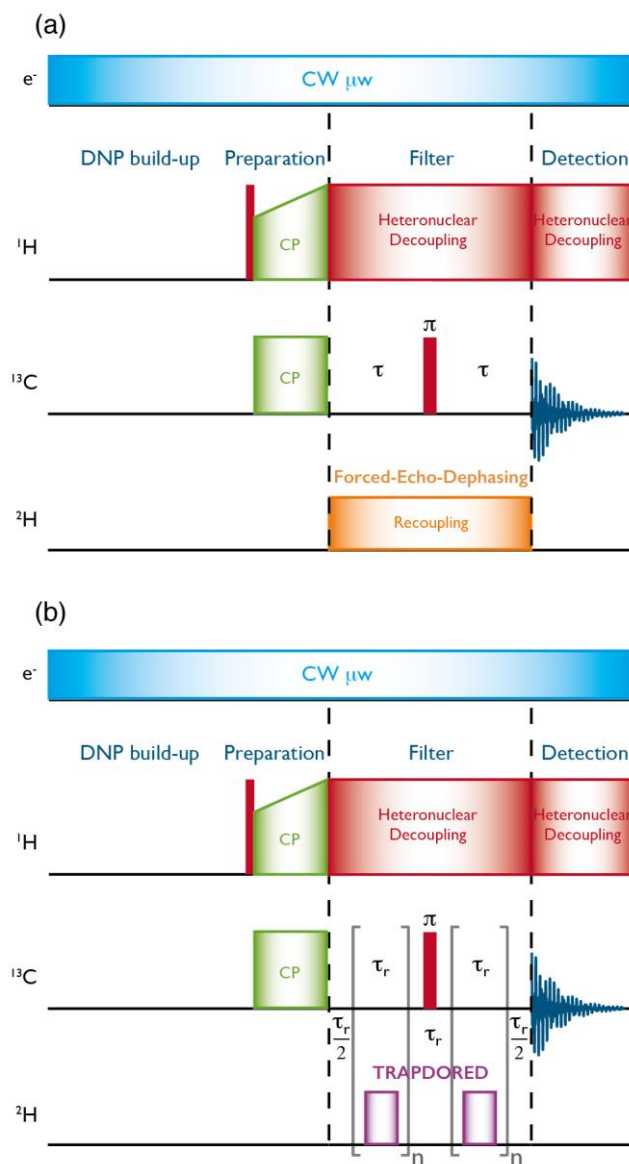
123 2.2. DNP-enhanced solid-state NMR experiments

124 Solid-state NMR experiments were recorded using a Bruker DNP-NMR AVANCE III 400
125 MHz (9.4 T) spectrometer equipped with a gyrotron and associated transmission line capable of
126 delivering ~ 5 W of ~ 264 GHz μ w irradiation at the sample.²⁷ All experiments were recorded with
127 a 3.2 mm HXY triple-resonance MAS probe (in $\lambda/4$ ¹H transmission mode) at $\nu_0(^1\text{H}) = 400.33$
128 MHz, corresponding to the maximum ¹H enhancement field position for AMUPol at $\nu_0(e^-) = 263.7$
129 GHz, with the X-channel tuned to $\nu_0(^{13}\text{C}) = 100.66$ MHz and the Y-channel tuned to $\nu_0(^2\text{H}) =$
130 61.45 MHz.

131 Figure 1 illustrates the NMR radio frequency (RF) pulse sequences used herein. ¹H $\pi/2$ and
132 SPINAL-64²⁸ heteronuclear decoupling were applied to induce a nutation frequency of 100 kHz.

133 ^{13}C π -pulses and CP spin-locking were at ~ 43 kHz with corresponding ramped (50–100%) ^1H
134 spin-locking at ~ 80 kHz (100%) to induce efficient CP transfer. For the recoupling of ^2H – ^{13}C
135 dipolar interactions, continuous ^2H RF irradiation was applied during a rotor-synchronized spin-
136 echo of total duration 2τ (Figure 1a) or as rotor-synchronized pulses of duration $\leq \tau_r$ ($\tau_r = 1/\nu_r$)
137 during a spin-echo with a total duration of $2\tau_r(n+1)$ (Figure 1b). The pulse sequence given in Figure
138 1a then results in a Forced Echo Dephasing experiment, or FEDex, and the sequence given in
139 Figure 1b a modified version of TRAPDOR,²⁵ here a TRAnSfer of Populations in DOuble
140 Resonance Echo Dephasing, or TRAPDORED, NMR. Note that in conventional TRAPDOR NMR
141 the RF irradiation applied to the quadrupolar spins is not usually applied in the second half of the
142 spin-echo.²⁹ For TRAPDORED NMR, optimum dephasing results are obtained with irradiation on
143 the quadrupolar nucleus (here ^2H) in both halves of the spin-echo.

144



145

146 **Figure 1. FEDex (a) and TRAPDORED (b) NMR pulse sequences.** After a DNP build-up
 147 period using suitable continuous wave (CW) μw irradiation, transverse ^{13}C magnetization is
 148 prepared through a cross-polarization step. Subsequently, a filter period is applied whereby ^2H -
 149 ^{13}C dipolar interactions are reintroduced to rapidly dephase ^{13}C signals from deuterated solvents,
 150 before detection of the remaining ^{13}C magnetization.

151

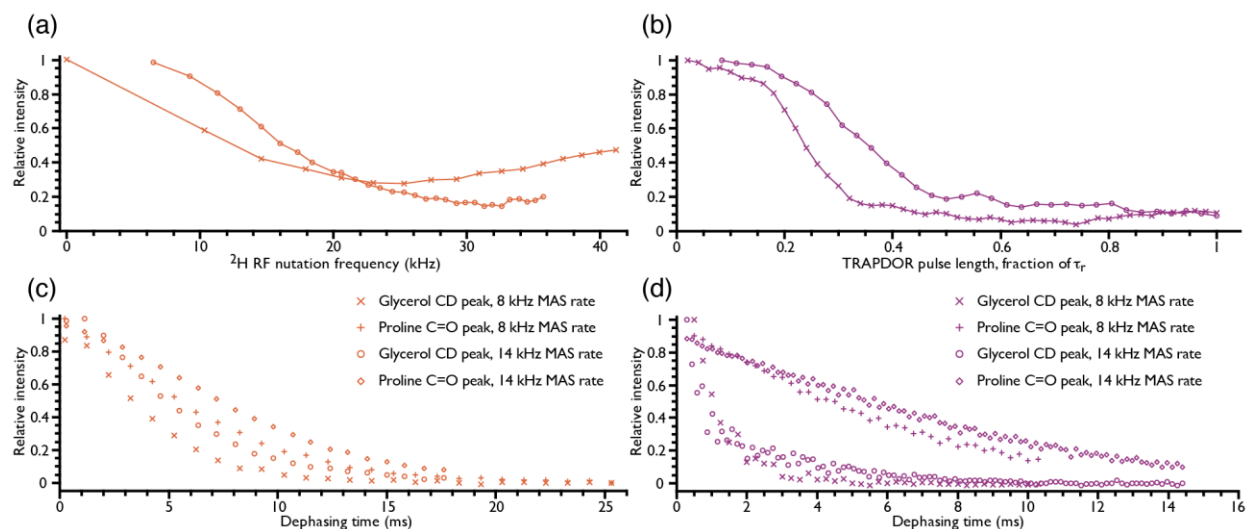
152 **3. Results and discussion**

153 3.1. Reintroducing the ^2H - ^{13}C dipolar interaction for forced signal dephasing

154 Under even moderate MAS rates, the dipolar interaction between ^2H and ^{13}C spins will be
155 effectively averaged to zero. Therefore, to produce dephasing of magnetization from ^{13}C nuclei in
156 close proximity to ^2H nuclei, the dipolar interaction needs to be reintroduced. Fittingly, a powerful
157 technique that reintroduces the dipolar interaction between spin-1/2 and quadrupolar nuclei under
158 MAS has been previously described.^{25,29,30} Figure 1 shows the NMR pulse sequences for the two
159 methods presented herein to dephase deuterated solvent signals and recover only the signals of
160 interest. Both methods rely on employing a filter period where unwanted signals are forcibly
161 dephased due to the reintroduction of a dipolar interaction to ^2H spins. The two methods differ in
162 the way in which they reintroduce this dipolar interaction during the filter period. The Forced Echo
163 Dephasing experiment, or FEDex, shown in Figure 1a uses continuous wave (CW) ^2H RF
164 irradiation during the filter period, whereas the TRAnsfer of Populations in DOuble Resonance
165 Echo Dephasing, or TRAPDORED, experiment shown in Figure 1b uses rotor-synchronized ^2H
166 RF pulses.

167 Figure 2 presents the experimental optimization of the variables associated with FEDex
168 and TRAPDORED. They are simple to set up, since both only rely on one main variable. For
169 FEDex, this variable is the RF power applied to the ^2H spins, which is MAS dependent (see Figure
170 2a). At the slower spinning rate of 8 kHz, the RF power required for optimum dephasing (i.e.,
171 smallest returned peak intensity) is lower than that at 14 kHz, indicating that the dipolar recoupling
172 is due to a matching of the nutation of the ^2H spins and the spinning rate (or integer multiple of).
173 Conversely, for TRAPDORED, the maximum possible RF power applied to the ^2H spins results
174 in the best dephasing (data not shown), as would be expected with TRAPDOR-type recoupling,²⁵

175 with the optimized variable being the pulse length. It is clear from Figure 2b that the
 176 TRAPDORED pulse length should be between $0.5\tau_r$ and τ_r . The dephasing efficiency is fairly
 177 robust to the offset frequency of the ^2H RF irradiation (± 8 kHz), with best performance slightly
 178 off resonance (+ 3 kHz) (see Figure S1 of the Supporting Information). Once FEDex and
 179 TRAPDORED have been optimized, then the required dephasing time can be obtained.



180
 181 **Figure 2. Optimization of FEDex (a, c) and TRAPDORED (b, d) pulse sequences.** The sample
 182 used was 2M *L*-proline in glycerol- d_8 /D $_2$ O/Htop $_2$ O with 10 mM AMUPol. The calibration was
 183 performed on the resulting relative ^{13}C intensity of the glycerol CD resonance at $\delta\{^{13}\text{C}\} = 72$ ppm
 184 and compared (in (c) and (d)) to the *L*-proline carboxyl ^{13}C resonance ($\delta\{^{13}\text{C}\} = 176$ ppm). A MAS
 185 rate of 8 kHz or 14 kHz and recycle delay of 3 s were used, along with total dephasing times of
 186 5.5 ms for (a) or 12.5 ms for (b). A ^2H RF nutation frequency of 36 kHz was used for the calibration
 187 shown in (b) and (d), whereas 23 and 33 kHz were used for the points measured in (c) at 8 kHz
 188 and 14 kHz MAS rates, respectively. Pulse lengths of $0.62\tau_r$ and $0.99\tau_r$ were used for the points
 189 measured in (d) at 8 kHz and 14 kHz MAS rates, respectively.

190

191 Figure 2c and Figure 2d show the relative intensity of the ^{13}C CD resonance of deuterated
192 glycerol ($\delta\{^{13}\text{C}\} = 72$ ppm, see Figure 3) and compare it to that of the *L*-proline carboxyl ($\delta\{^{13}\text{C}\}$
193 $= 176$ ppm, see Figure 3) from a frozen solution of 2M *L*-proline, 10 mM AMUPol, and glycerol-
194 $\text{d}_8/\text{D}_2\text{O}/\text{H}_2\text{O}$ as a function of the filter period duration (dephasing time), recorded using the
195 (optimized) pulse sequences from Figure 1a and Figure 1b, respectively. Instantly, it is evident
196 that TRAPDORED gives better results. For the two MAS rates tested (8 and 14 kHz), there is a
197 greater intensity difference between the unwanted (CD) and wanted (carboxyl) peaks using
198 TRAPDORED. This means that the dephasing is more efficient with this technique. At 8 kHz
199 MAS rate, 5.5 ms of TRAPDORED are required for there to be negligible remaining intensity of
200 the solvent peak, whereas over twice this dephasing time is needed for the same result with FEDex.
201 Therefore, the desired (*L*-proline) signal will be more intense following TRAPDORED, while the
202 solvent signal is suppressed adequately. Note that the proportion of the remaining, desired signal
203 depends on the apparent time constant for transverse signal decay under a refocusing echo, T_2' , for
204 the particular resonance. In the case of the *L*-proline carboxyl, 42 % of the signal remains after an
205 echo of 5.5 ms total duration compared to that obtained with a similar experiment recorded without
206 the filter period. It should be highlighted though that the $^{13}\text{C}T_2'$ for small molecules dissolved in
207 frozen glycerol/water solutions that contain paramagnetic polarizing agents suitable for MAS-
208 DNP is generally short (and depends on the concentration of the polarizing agent).¹¹ Moreover,
209 there will be a non-negligible recoupling of the ^2H - ^{13}C dipolar interaction between the abundant
210 glycerol deuterons and the ^{13}C of *L*-proline owing to the dilution of the analyte, which will also
211 induce a shorter apparent $^{13}\text{C}T_2'$. Therefore, and as shown below, bulk systems such as crystalline
212 solids that are not as detrimentally impacted by the presence of the paramagnets or recoupling can

213 retain long $^{13}\text{C}T_2'$ values, resulting in the acquisition of desired signals with almost negligible
214 intensity losses, while completely suppressing solvent signals, via FEDex or TRAPDORED NMR.

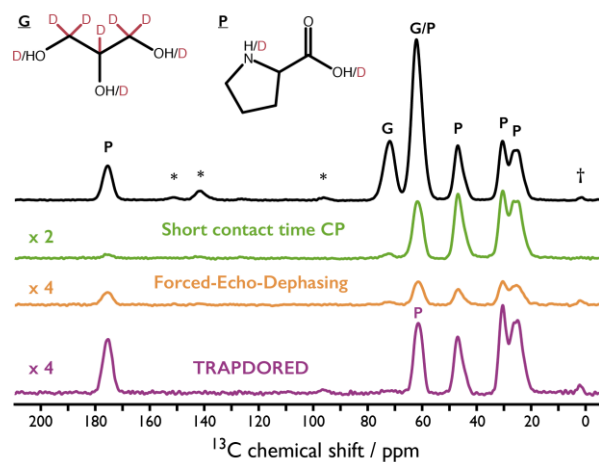
215 It can also be seen from Figure 2c and Figure 2d that faster sample spinning has a
216 detrimental effect on the efficacy of both dephasing methods, with more relative intensity of the
217 glycerol peak remaining after equivalent dephasing times. Thus, longer dephasing times are
218 required to completely suppress deuterated solvent signals, which could lead to reduced remaining
219 intensity of the desired signals. However, it is also known that faster sample spinning can also
220 increase T_2' values in MAS-DNP experiments,³¹ so the losses from desired signals will be less
221 significant. For the example from Figure 2d, 8.8 ms of TRAPDORED at a MAS rate of 14 kHz
222 are required for there to be negligible remaining intensity of the solvent peak, leaving 34 % of the
223 intensity for the desired peak compared to a similar experiment recorded without the filter period.
224 Faster sample spinning reduces the probability of transitions between the energy levels in the
225 quadrupolar ^2H nuclei under irradiation, reducing the TRAPDOR recoupling effect.²⁵ This is due
226 to the irradiation not fully inducing adiabatic population transfers between the Zeeman levels of
227 the ^2H nuclei.²⁵ Therefore, FEDex could be the better choice at higher spinning rates (> 20 kHz).

228

229 3.2. Frozen solution of *L*-proline at natural isotopic abundance

230 Taking the optimized variables and dephasing times from Figure 2 that successfully
231 suppress the ^{13}C signals from the deuterated solvent, DNP-enhanced FEDex and TRAPDORED
232 NMR spectra of *L*-proline in glycerol- $\text{d}_8/\text{D}_2\text{O}/\text{H}_2\text{O}$ were recorded. *L*-proline was chosen because
233 it has an overlapping ^{13}C resonance with one of the two glycerol ^{13}C peaks (at $\delta\{^{13}\text{C}\} = 62$ ppm).
234 Figure 3 shows these FEDex and TRAPDORED spectra and compares them to corresponding CP
235 spectra. It is clear that both FEDex and TRAPDORED effectively suppress the solvent (glycerol)

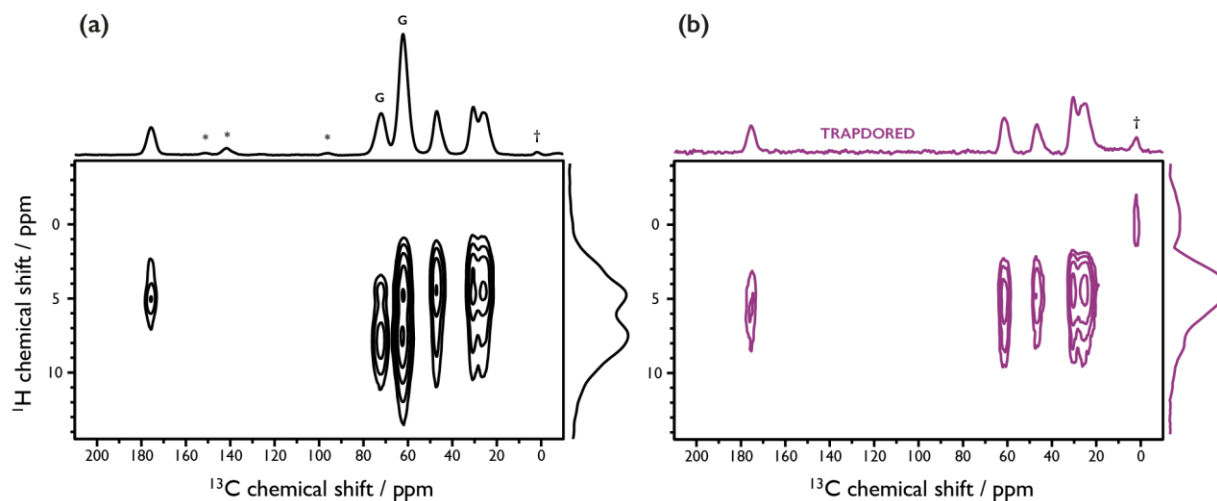
236 ^{13}C signals, albeit with intensity losses for the analyte (*L*-proline) – moreso with FEDex than
 237 TRAPDORED. These methods then reveal the *L*-proline ^{13}C resonance at $\delta\{^{13}\text{C}\} = 62$ ppm, which
 238 was previously obscured by a glycerol ^{13}C peak. As shown in Figure 3, a $\{^1\text{H}-\}^{13}\text{C}$ CP MAS
 239 experiment that uses a short CP contact time (50 μs) can also be used to suppress the glycerol ^{13}C
 240 signals, since the corresponding nuclei are far from ^1H nuclei. However, it does not do so
 241 completely, and a short CP contact time will also dramatically reduce the intensity of desired ^{13}C
 242 peaks in the analyte that are not directly bonded to ^1H , as can be seen from the almost negligible
 243 intensity of the carboxyl peak of *L*-proline in Figure 3 (at $\delta\{^{13}\text{C}\} = 176$ ppm).



244
 245 **Figure 3. DNP-enhanced ^{13}C NMR spectra of *L*-proline (P, inset) in glycerol- d_8 (G,**
 246 **inset)/D $_2$ O/H $_2$ O with 10 mM AMUPol biradical polarizing agent, recorded using a recycle delay**
 247 **of 3 s, a MAS rate of 8 kHz, a sample temperature of ~ 100 K, and at a magnetic field strength of**
 248 **9.4 T. A $\{^1\text{H}-\}^{13}\text{C}$ CP MAS NMR spectrum recorded with a CP contact time of 2 ms (black) is**
 249 **compared to a similar spectrum recorded with a CP contact time of 50 μs (green) and FEDex**
 250 **(orange) and TRAPDORED (purple) spectra, both recorded using a CP step with contact time 2**
 251 **ms. The FEDex and TRAPDORED times were 12.5 and 5.5 ms, respectively. Asterisks (*) and**

252 daggers (†) denote spinning side bands and signals from a silicone plug, respectively. Note the
253 factors highlighting the change in scale of the spectra.

254
255 The filter periods from Figure 1a and Figure 1b, representing the FEDex and TRAPDORED parts
256 of the NMR pulse sequence, respectively, can be combined with any solid-state NMR experiment
257 (so long as there are a sufficient number of available RF channels), allowing the suppression of
258 resonances from molecules containing quadrupolar spins. Figure 4 presents DNP-enhanced two-
259 dimensional ^1H - ^{13}C dipolar correlation spectra of the *L*-proline sample, which have been recorded
260 with (Figure 4b) and without (Figure 4a) the inclusion of ^2H TRAPDORED into the pulse
261 sequence. Instantly, it is evident in Figure 4a that there are large cross-peaks stemming from the
262 glycerol (labelled 'G' in the figure), whereas these are not present in Figure 4b, owing to the use
263 of TRAPDORED. Not only do these glycerol resonances obscure information in the ^{13}C
264 dimension, but also in the ^1H dimension. Although the ^{13}C nuclei of the deuterated glycerol are
265 not directly bonded to ^1H nuclei, they still experience a dipolar interaction with those that are
266 sufficiently close (e.g., from H_2O in the solvent mixture), resulting in the dominating cross-peaks,
267 even at the relatively short mixing time used (250 μs). The ^1H dimension of DNP-enhanced ^1H -
268 ^{13}C dipolar correlation spectra has proven especially useful in the atomic-scale characterization of
269 functionalized surfaces,³ so it is extremely important that this remains as free from overlapping
270 solvent signals as the ^{13}C dimension.



271

272 **Figure 4. DNP-enhanced ^1H - ^{13}C FSLG-HETCOR³² spectra of *L*-proline in glycerol-**
 273 **$\text{d}_8/\text{D}_2\text{O}/\text{H}_2\text{O}$ with 10 mM AMUPol biradical polarizing agent, recorded using a recycle delay of 3**
 274 **s, a MAS rate of 8 kHz, a sample temperature of ~ 100 K, and at a magnetic field strength of 9.4**
 275 **T. A standard ^1H - ^{13}C FSLG-HETCOR spectrum (a) is compared to a TRAPDORED version (b),**
 276 **both recorded with CP contact times of 500 μs . Also shown, skyline projections taken parallel to**
 277 **the ^1H dimension (right) and corresponding ^{13}C spectra from Figure 3 (top). Asterisks (*) and**
 278 **daggers (†) denote spinning side bands and signals from a silicone plug, respectively.**

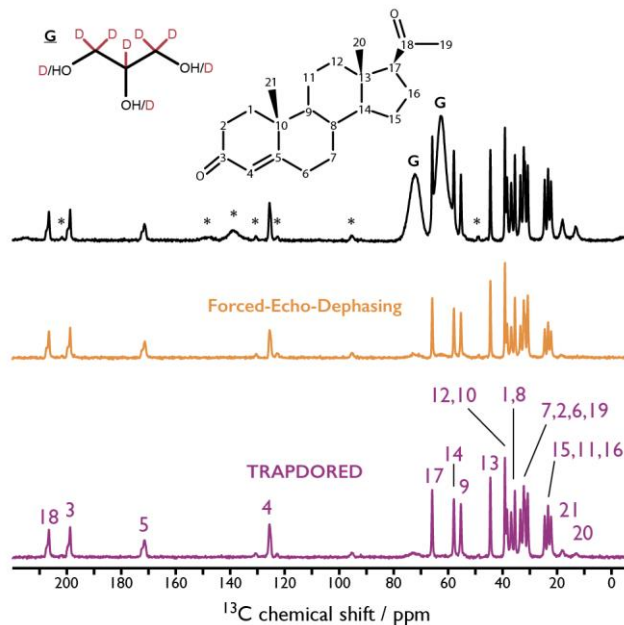
279

280 **3.3. Powdered progesterone at natural isotopic abundance**

281 Above, FEDex and TRAPDORED were validated on a *L*-proline frozen solution. There,
 282 the intensity losses of the desired signals will be maximized due to their short T_2' values induced
 283 by the close proximity of paramagnets to the analyte. Therefore, it is interesting to also demonstrate
 284 the usefulness of these methods on a characteristic 'real' analyte, such as a bulk solid that may
 285 then not be as negatively impacted by the presence of paramagnets. MAS-DNP has recently be

286 shown to be immensely valuable for the study of this type of system.^{7,8,33,34} Of particular note is
287 the application towards pharmaceutical compounds.³⁵ Along these lines, Figure 5 shows a DNP-
288 enhanced $\{^1\text{H}-\}^{13}\text{C}$ CPMAS NMR spectrum of microcrystalline progesterone. The sample
289 preparation, requiring the addition of a glycerol- d_8 /D₂O/H₂O solvent matrix to allow dispersal of
290 the polarizing agent and efficient hyperpolarization of the progesterone, results in large glycerol
291 peaks in the $\{^1\text{H}-\}^{13}\text{C}$ CPMAS NMR spectrum that overlap with signals from the progesterone.
292 Also shown in Figure 5 are corresponding spectra that have been recorded with the pulse sequences
293 in Figure 1a and Figure 1b, giving FEDex and TRAPDORED spectra, respectively. The solvent
294 peaks have been effectively suppressed in these spectra. Moreover, there are only small or
295 negligible signal losses from the analyte. This is because the $^{13}\text{C}T_2'$ of the progesterone is relatively
296 long, since most of this analyte's nuclei are far from the exogenous paramagnets or ^2H nuclei.

297 The absolute sensitivity ratio (ASR)⁷ for the DNP-enhanced experiment was measured in
298 the usual manner by comparing the optimum signal-to-noise (S/N) ratio per unit square root of
299 time for the DNP-enhanced $\{^1\text{H}-\}^{13}\text{C}$ CPMAS NMR spectrum to the corresponding spectrum
300 recorded under conventional means (9.4 T, ambient temperature, fully packed 3.2 mm thin-walled
301 zirconia rotor with pure (no solvent or polarizing agent) progesterone powder; data not shown).
302 Here, the ASR = 6. Because the ASR uses a comparison to a conventional experiment, then both
303 the positive and negative effects from performing MAS-DNP experiments are accounted for.³⁶ An
304 ASR = 6 corresponds to being able to record experiments 36 times faster. Note that previously,
305 using conventional solid-state NMR, 10 days of experimental time was required to record a ^{13}C
306 homonuclear correlation spectrum of progesterone at its natural isotopic abundance.³⁷ The
307 combination of MAS-DNP and spectral editing, in the form of FEDex or TRAPDORED, therefore
308 allows the fast and undisturbed characterization of analytes.



309
 310 **Figure 5. DNP-enhanced $\{^1\text{H}\}\text{-}^{13}\text{C}$ CP MAS NMR spectra of progesterone**, wetted with 10
 311 mM AMUPol biradical polarizing agent in glycerol- $\text{d}_8/\text{D}_2\text{O}/\text{H}_2\text{O}$, recorded using a recycle delay
 312 of 8.5 s, a MAS rate of 7.7 kHz, a sample temperature of ~ 100 K, and at a magnetic field strength
 313 of 9.4 T. A $\{^1\text{H}\}\text{-}^{13}\text{C}$ CP MAS NMR spectrum (black, top) is compared to FEDex (orange, middle)
 314 and TRAPDORED (purple, bottom) spectra, all recorded using a CP step with contact time 2 ms.
 315 The FEDex and TRAPDORED times were 12.9 and 3.6 ms, respectively. Asterisks (*) denote
 316 spinning side bands.

317

318 4. Conclusions

319 Two methods have been presented that force the suppression of solvent signals in common
 320 MAS-DNP experiments. These two methods, named FEDex and TRAPDORED, are simple to set
 321 up and can be easily combined with established solid-state NMR experiments. They both work
 322 through the reintroduction of the heteronuclear dipolar interaction between ^{13}C spins from the DNP

323 solvent, the presence of which can cause overwhelming signals from associated resonances in ^{13}C
324 NMR spectra, and nearby quadrupolar spins, resulting in fast dephasing of these ^{13}C resonances.
325 The utility of these two methods has been demonstrated for samples containing deuterated glycerol
326 as part of the DNP solvent mixture and for analytes in frozen solution as well as in powdered form.
327 It was shown that TRAPDORED delivers better efficiency than FEDex for solvent suppression
328 under the experimental conditions used here.

329 It should be highlighted that these methods are not restricted to suppressing signals from
330 glycerol- d_8 and are suitable for other deuterated DNP solvents, many of which have shown useful
331 properties for MAS-DNP studies (such as dimethylsulfoxide- d_6 /water,³⁸ 1,1,2,2-tetrachloroethane-
332 d_2 ,³⁹ and ortho-terphenyl- d_{14} ⁴⁰). Moreover, the methods proposed herein could also be applied to
333 prevalent non-deuterated MAS-DNP solvents such as 1,1,2,2-tetrachloroethane³ and 1,1,2,2-
334 tetrabromoethane,³⁸ where ^{35}Cl or ^{81}Br irradiation could be used instead of ^2H irradiation to
335 suppress signals stemming from these solvents, respectively. Finally, the methods demonstrated
336 herein for solvent suppression can also be useful for spectral editing and resonance assignment in
337 conventional solid-state MAS NMR spectroscopy of other systems that contain quadrupolar nuclei
338 in high isotopic abundance, such as ^7Li , ^{14}N , and ^{27}Al .

339

340

341

342

343

344 **Corresponding Author**

345 *E-mail: gael.depaepe@cea.fr

346

347 **Acknowledgements**

348 This work was supported by the French National Research Agency through the Labex
349 ARCANÉ (ANR-11-LABX-0003-01), the “programme blanc” (ANR-12-BS08-0016-01), and the
350 European Research Council (ERC-CoG-2015, No. 682895). The RTB is acknowledged for
351 financial support.

352

353 **References**

354 (1) Hall, D. A.; Maus, D. C.; Gerfen, G. J.; Inati, S. J.; Becerra, L. R.; Dahlquist, F. W.; Griffin, R. G. *Science*
355 **1997**, *276*, 930–932.

356 (2) Ni, Q. Z.; Daviso, E.; Can, T. V.; Markhasin, E.; Jawla, S. K.; Swager, T. M.; Temkin, R. J.; Herzfeld, J.;
357 Griffin, R. G. *Acc. Chem. Res.* **2013**, *46*, 1933–1941.

358 (3) Rossini, A. J.; Zagdoun, A.; Lelli, M.; Lesage, A.; Copéret, C.; Emsley, L. *Acc. Chem. Res.* **2013**, *46*, 1942–
359 1951.

360 (4) Andrew, E. R.; Bradbury, A.; Eades, R. G. *Nature* **1959**, *183*, 1802–1803.

361 (5) Overhauser, A. *Phys. Rev.* **1953**, *92*, 411–415.

362 (6) Carver, T. R.; Slichter, C. P. *Phys. Rev.* **1953**, *92*, 212–213.

363 (7) Takahashi, H.; Lee, D.; Dubois, L.; Bardet, M.; Hediger, S.; De Paëpe, G. *Angew. Chem. Int. Ed. Engl.* **2012**,
364 *51*, 11766–11769.

365 (8) Rossini, A. J.; Zagdoun, A.; Hegner, F.; Schwarzwälder, M.; Gajan, D.; Copéret, C.; Lesage, A.; Emsley, L.

- 366 *J. Am. Chem. Soc.* **2012**, *134*, 16899–16908.
- 367 (9) Märker, K.; Pingret, M.; Mouesca, J.-M.; Gasparutto, D.; Hediger, S.; De Paëpe, G. *J. Am. Chem. Soc.* **2015**,
368 *137*, 13796–13799.
- 369 (10) Lee, D.; Monin, G.; Duong, N. T.; Zamanillo Lopez, I.; Bardet, M.; Mareau, V.; Gonon, L.; De Paëpe, G. *J.*
370 *Am. Chem. Soc.* **2014**, *136*, 13781–13788.
- 371 (11) Takahashi, H.; Fernández-de-Alba, C.; Lee, D.; Maurel, V.; Gambarelli, S.; Bardet, M.; Hediger, S.; Barra,
372 A.-L.; De Paëpe, G. *J. Magn. Reson.* **2014**, *239*, 91–99.
- 373 (12) Zagdoun, A.; Rossini, A. J.; Gajan, D.; Bourdolle, A.; Ouari, O.; Rosay, M.; Maas, W. E.; Tordo, P.; Lelli,
374 M.; Emsley, L.; Lesage, A.; Copéret, C. *Chem. Commun. (Camb)*. **2012**, *48*, 654–656.
- 375 (13) Song, C.; Hu, K.-N.; Joo, C.-G.; Swager, T. M.; Griffin, R. G. *J. Am. Chem. Soc.* **2006**, *128*, 11385–11390.
- 376 (14) Ong, T.; Mak-Jurkauskas, M. L.; Walish, J. J.; Michaelis, V. K.; Corzilius, B.; Smith, A. A.; Clausen, A. M.;
377 Cheetham, J. C.; Swager, T. M.; Griffin, R. G. *J. Phys. Chem. B* **2013**, *117*, 3040–3046.
- 378 (15) Michaelis, V. K.; Ong, T.-C.; Kieseewetter, M. K.; Frantz, D. K.; Walish, J. J.; Ravera, E.; Luchinat, C.;
379 Swager, T. M.; Griffin, R. G. *Isr. J. Chem.* **2014**, *54*, 207–221.
- 380 (16) Bouleau, E.; Saint-Bonnet, P.; Mentink-Vigier, F.; Takahashi, H.; Jacquot, J.-F.; Bardet, M.; Aussenac, F.;
381 Pureau, A.; Engelke, F.; Hediger, S.; Lee, D.; De Paëpe, G. *Chem. Sci.* **2015**, *6*, 6806–6812.
- 382 (17) Potapov, A.; Yau, W.-M.; Tycko, R. *J. Magn. Reson.* **2013**, *231*, 5–14.
- 383 (18) Ravera, E.; Corzilius, B.; Michaelis, V. K.; Luchinat, C.; Griffin, R. G.; Bertini, I. *J. Phys. Chem. B* **2014**,
384 *118*, 2957–2965.
- 385 (19) Takahashi, H.; Hediger, S.; De Paëpe, G. *Chem. Commun. (Camb)*. **2013**, *49*, 9479–9481.
- 386 (20) De Vita, E.; Frydman, L. *J. Magn. Reson.* **2001**, *148*, 327–337.
- 387 (21) Zheng, G.; Price, W. S. *Prog. Nucl. Magn. Reson. Spectrosc.* **2010**, *56*, 267–288.

- 388 (22) Romanenko, I.; Gajan, D.; Sayah, R.; Crozet, D.; Jeanneau, E.; Lucas, C.; Leroux, L.; Veyre, L.; Lesage, A.;
389 Emsley, L.; Lacôte, E.; Thieuleux, C. *Angew. Chem. Int. Ed. Engl.* **2015**, *54*, 12937–12941.
- 390 (23) Schmidt-Rohr, K.; Fritzsching, K. J.; Liao, S. Y.; Hong, M. *J. Biomol. NMR* **2012**, *54*, 343–353.
- 391 (24) Gullion, T.; Schaefer, J. *J. Magn. Reson.* **1989**, *81*, 196–200.
- 392 (25) Grey, C. P.; Vega, A. J. *J. Am. Chem. Soc.* **1995**, *117*, 8232–8242.
- 393 (26) Sauvée, C.; Rosay, M.; Casano, G.; Aussenac, F.; Weber, R. T.; Ouari, O.; Tordo, P. *Angew. Chem. Int. Ed.*
394 *Engl.* **2013**, *52*, 10858–10861.
- 395 (27) Rosay, M.; Tometich, L.; Pawsey, S.; Bader, R.; Schauwecker, R.; Blank, M.; Borchard, P. M.; Cauffman, S.
396 R.; Felch, K. L.; Weber, R. T.; Temkin, R. J.; Griffin, R. G.; Maas, W. E. *Phys. Chem. Chem. Phys.* **2010**, *12*,
397 5850–5860.
- 398 (28) Fung, B. M.; Khitrin, A. K.; Ermolaev, K. *J. Magn. Reson.* **2000**, *142*, 97–101.
- 399 (29) Grey, C. P.; Veeman, W. S.; Vega, A. J. *J. Chem. Phys.* **1993**, *98*, 7711.
- 400 (30) Grey, C. P.; Veeman, W. S. *Chem. Phys. Lett.* **1992**, *192*, 379–385.
- 401 (31) Chaudhari, S. R.; Berruyer, P.; Gajan, D.; Reiter, C.; Engelke, F.; Silverio, D. L.; Copéret, C.; Lelli, M.;
402 Lesage, A.; Emsley, L. *Phys. Chem. Chem. Phys.* **2016**, *18*, 10616–10622.
- 403 (32) van Rossum, B.-J.; Förster, H.; de Groot, H. J. M. *J. Magn. Reson.* **1997**, *124*, 516–519.
- 404 (33) Blanc, F.; Chong, S. Y.; McDonald, T. O.; Adams, D. J.; Pawsey, S.; Caporini, M. A.; Cooper, A. I. *J. Am.*
405 *Chem. Soc.* **2013**, *135*, 15290–15293.
- 406 (34) Rossini, A. J.; Schlagnitweit, J.; Lesage, A.; Emsley, L. *J. Magn. Reson.* **2015**, *259*, 192–198.
- 407 (35) Rossini, A. J.; Widdifield, C. M.; Zagdoun, A.; Lelli, M.; Schwarzwälder, M.; Copéret, C.; Lesage, A.;
408 Emsley, L. *J. Am. Chem. Soc.* **2014**, *136*, 2324–2334.
- 409 (36) Lee, D.; Hediger, S.; De Paëpe, G. *Solid State Nucl. Magn. Reson.* **2015**, *66–67*, 6–20.

410 (37) Lee, D.; Struppe, J.; Elliott, D. W.; Mueller, L. J.; Titman, J. J. *Phys. Chem. Chem. Phys.* **2009**, *11*, 3547–
411 3553.

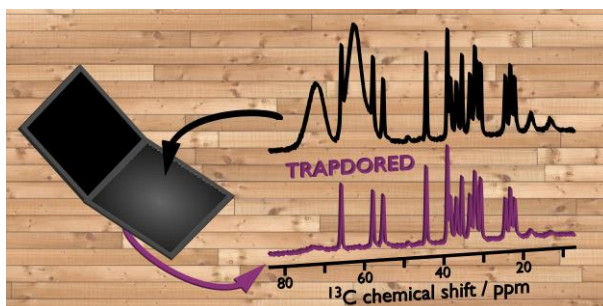
412 (38) Lee, D.; Duong, N. T.; Lafon, O.; De Paëpe, G. *J. Phys. Chem. C* **2014**, *118*, 25065–25076.

413 (39) Le, D.; Casano, G.; Phan, T. N. T.; Ziarelli, F.; Ouari, O.; Aussenac, F.; Thureau, P.; Mollica, G.; Gimes, D.;
414 Tordo, P.; Viel, S. *Macromolecules* **2014**, *47*, 3909–3916.

415 (40) Lelli, M.; Chaudhari, S. R.; Gajan, D.; Casano, G.; Rossini, A. J.; Ouari, O.; Tordo, P.; Lesage, A.; Emsley,
416 L. *J. Am. Chem. Soc.* **2015**, *137*, 14558–14561.

417

418 **For Table of Contents Only**



419

420